XLVI CILAMCE
VITÓRIA - ES - BRAZIL - 2025
XLVI IBERO-LATIN AMERICAN CONGRESS ON COMPUTATIONAL METHODS IN ENGINEERING

Numerical analysis of external diaphragm connection between I-beam and circular tubular column

Rodrigo Roger Daré Uliana[1] e Macksuel Soares de Azevedo[2]*

[1]*Dept. of Civil Engineering, Federal University of Espírito Santo*
Av. Fernando Ferrari, 514, Campus Goiabeiras, Vitória, ES. CEP 29.075-910. Brasil
rodrigouliana.eng@gmail.com

[2]*Dept. of Civil Engineering, Federal University of Espírito Santo*
Av. Fernando Ferrari, 514, Campus Goiabeiras, Vitória, ES. CEP 29.075-910. Brasil
macksuel.azevedo@ufes.br

Abstract. This paper addresses the structural behavior of the connection between circular hollow steel columns and I-beams in civil construction. As a strategy to improve the stiffness of this connection, external diaphragms are used, which are flat components integrated into the interface between the column and the beam. Notably, the Brazilian standard ABNT NBR 16239:2013 [1] does not cover the design of this type of connection. The objective of this study is to numerically analyze the behavior of welded connections between circular hollow section columns and I-section beams, using external diaphragms in X-type and XX-type configurations. These connections were subjected to axial and bending loads, with variations in column diameter and wall thickness also considered. The numerical modeling was performed using the finite element method and showed agreement with both numerical and experimental results obtained by Winkel (1998) [2]. The performance of the external diaphragm proved satisfactory, as it significantly increased stiffness and improved the connection's load-bearing capacity, as well as with the increase in column diameter and wall thickness.

Keywords: External diaphragm, steel structures, circular hollow section column, steel connections, numerical analysis.

1 Introduction

The connection between circular hollow section columns and I-section beams is widely used in civil construction and engineering projects, commonly found in large structures, bridges, and offshore platforms. This combination of structural elements allows the absorption of compressive, tensile, and bending loads, as well as the efficient transmission of these forces to the connection region. However, the efficiency and safety of these structures depend significantly on the stiffness of the beam-column connection.

The connection studied in this work is formed by welding I-beams to circular hollow section columns. Axial forces and bending moments acting at the joint region are considered to better understand the structural behavior of this configuration. Pereira (2013) [3] and Orrico (2018) [4] and note that the diaphragm is a connecting device in which a steel plate wraps around the column and connects to the beams to increase strength and stiffness, as well as to redistribute stresses caused by the beams, reducing stress and deformation in the columns.

2 Validação do modelo numérico

2.1 Winkel's Experiment (1998)

Winkel (1998) [2] conducted an experimental investigation to gather detailed information for calibrating numerical models. The data includes measurements of geometric and material properties, stress-strain or moment-

rotation curves, and observations of failure modes. The goal of this validation is to align the numerical models with experimental findings, presenting test plans for Series 2, which included combinations of loads on multiplanar joints using I-beams (IPE 240 or IPE 360) and circular hollow section (CHS) columns (Ø 324 x 9.5 mm).

The series comprised three tests investigating I-beam to CHS column connections under axial loading. In the joint between the I-beam and the column, the web was removed to isolate and analyze the flange contribution. It is important to note that, compared to practical applications, these tests were performed on reduced-scale models (approximately 1/3 of full size).

2.2 Numerical Model

A 3D model was used for numerical analysis via the finite element software ANSYS (2023). Coutinho (2015) [5] recommends the use of large displacement formulations when buckling and large deformations are expected. For solving the equilibrium equations, the full Newton-Raphson method was adopted to account for structural nonlinearities. According to Orrico (2018) [4], the beam consists of flanges and web plates, while the column behaves like a shell element due to its geometry. Therefore, the Shell181 element from ANSYS 23.0 was used, based on the Mindlin-Reissner theory, suitable for thin to moderately thick plates, and ideal for the beam and column configuration in this study.

2.3 Axial Force vs. Displacement Curves

The numerical analysis results were compared to those from Winkel (1998) [2], using axial force vs. displacement curves for the tested connections. The simulations applied shell elements (Shell181) to represent the welded joint. Figures 1(a) and 1(b) compare experimental and numerical results. Model 2C1 (Figure 1(a)) shows strong agreement with Winkel's results. However, model 2C3 (Figure 1(b)) presented significant discrepancies, even when compared to Winkel's own numerical findings.

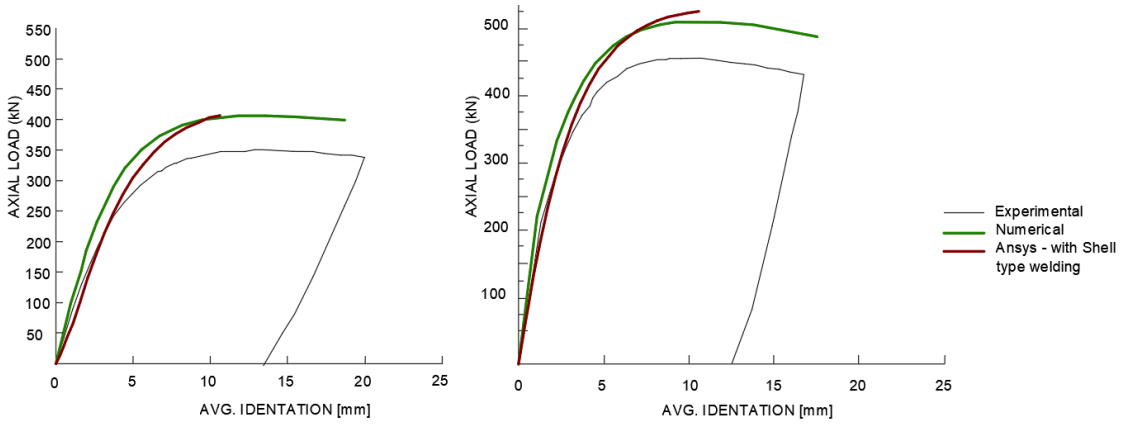


Figure 1. Axial force vs. displacement

2.4 Maximum connection capacity

Table 1 summarizes the differences between the values of the ultimate axial forces obtained in the analyses performed and presents a quantitative comparison with different connection configurations.

After validation, the external diaphragm was added to the model to evaluate its influence on the transmission of forces from the beam. Orrico (2018) [4] examined variations in diaphragm width and thickness. In this study, only one diaphragm model was adopted, within the limits set by Kurobane *et al*. (2004) [6].

Table 1 Comparison between numerical and experimental axial force capacity in Series 3 tests

MODEL	N_u(kN)		
	Experimental Winkel	Numeric Winkel	Ansys
2C1	245,3	350,6	340,46
2C3	325,0	456,0	408,23

3 Connection with external diaphragm

3.1 Combined bending moment and axial load

As seen in Figure 2, models with diaphragms showed improved performance, supporting loads with minimal displacement at the column face. Models 2C1 and 2C3 had average indentation below 5 mm, indicating significantly increased stiffness compared to the non-diaphragm versions.

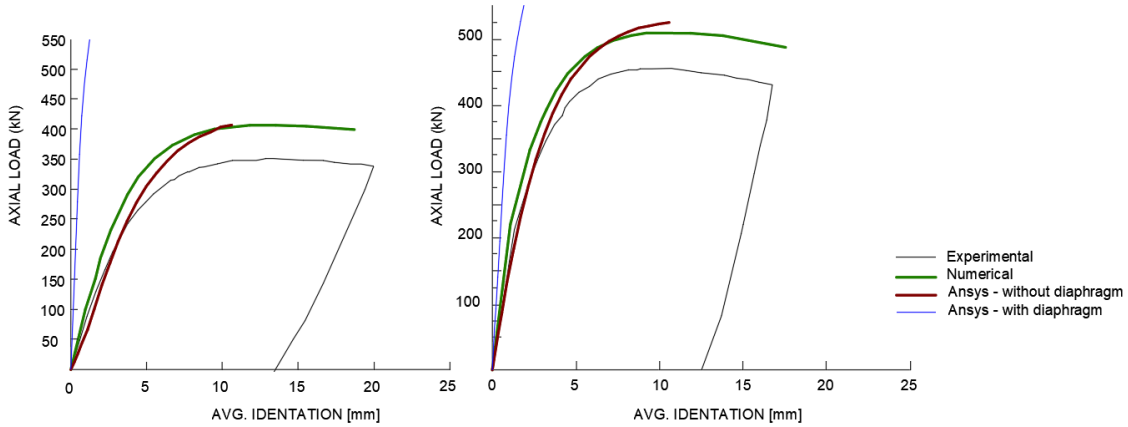


Figure 2. Axial force vs. displacement curves

3.2 Combined bending moment and axial load

To simulate more realistic structural conditions, a vertical load was applied at the beam's free end, generating a bending moment at the joint. The objective was to evaluate the column's behavior under combined loading. Figures 3(a) and 3(b) show axial force vs. displacement for models 2C1 and 2C3 with added bending moment. The diaphragm-equipped models clearly demonstrated greater load capacity and stiffness.

.

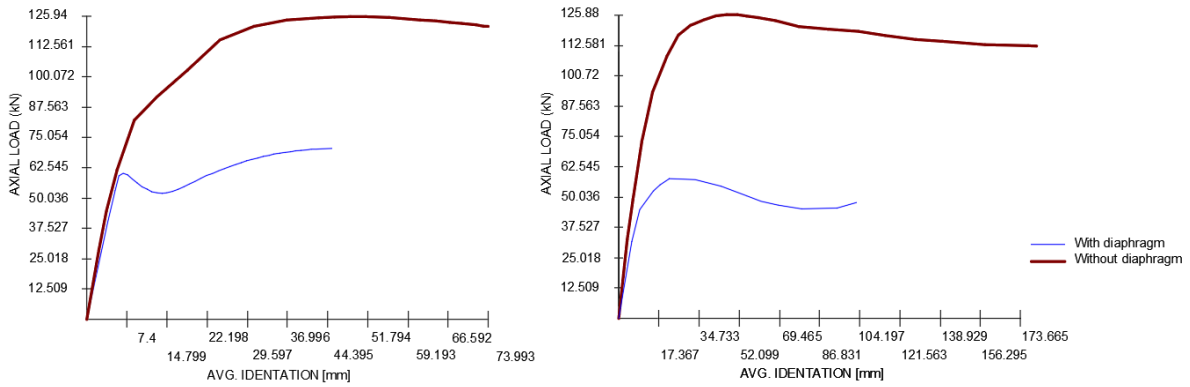


Figure 3. Axial force vs. displacement curves

3.3 Failure modes and Von Mises stresses

Figures 4 and 5 illustrate failure modes via Von Mises stress criteria. All models without diaphragms failed due to plastification at the column face. In diaphragm-equipped models, plastification occurred both in the column and in the diaphragm.

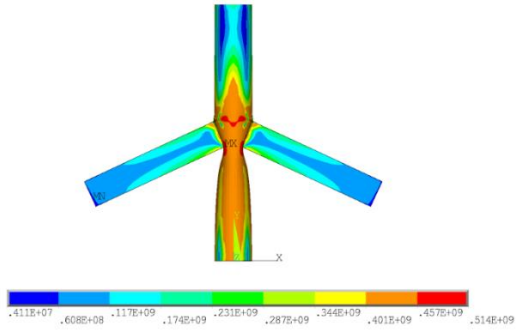


Figure 4. Plastification in column without diaphragm

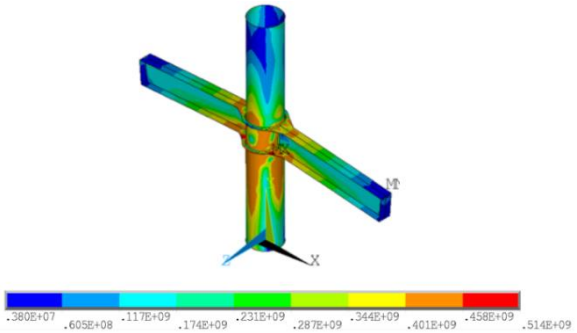


Figure 5. Plastification in column with diaphragm

3.4 Bending moment capacity at the connection

A separate analysis focused on the bending resistance at the XX-type joint, as proposed by Orrico (2018) [4]. Variations in commercial wall thicknesses (7.1 mm to 14.2 mm) and diameters (244.48 mm to 355.6 mm) were tested (Table 2). A total of 40 models were analyzed.

Table 2. Combinations of column diameter and thickness (mm)

DIAMETER	THICKNESS									
244,48 273 323,8 355,6	7,10	8,00	8,80	9,65	10,00	11,00	11,65	12,50	13,06	14,20

The applied load generated a bending moment at the beam's end. As wall thickness increased, so did bending resistance, as seen in Figure 6. The failure mode was consistent across models, indicating a behavioral trend.

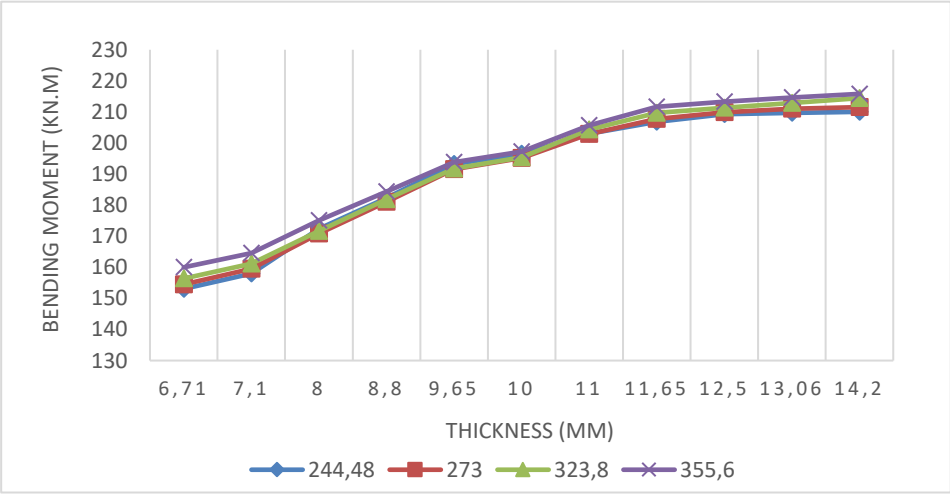


Figure 6. Bending moment vs. wall thickness for different models

3.5 Moment-rotation curves

Moment vs. rotation curves confirmed consistency with the bending resistance results. Figures 7 and 8 present curves for thicknesses of 7.1 mm, 10 mm, and 14.2 mm, chosen to prevent overlapping.

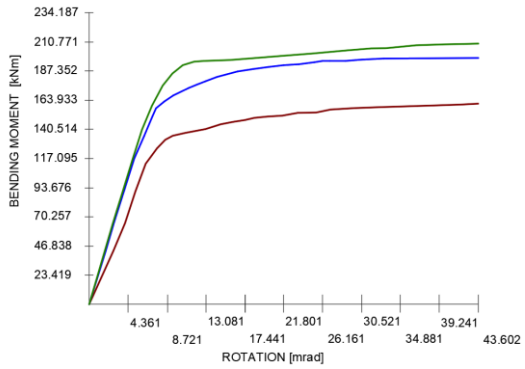


Figure 7. Moment-rotation curve for 244.48 mm diameter

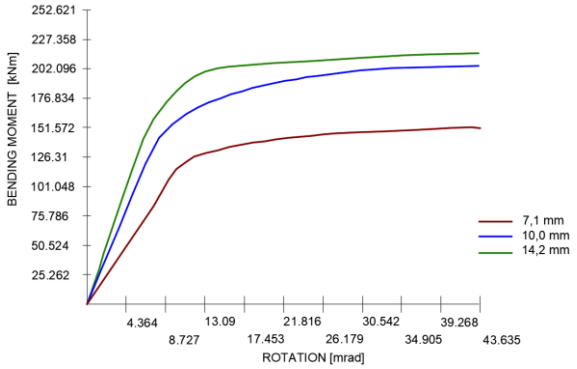


Figure 8. Moment-rotation curve for 355.6 mm diameter

3.6 Failure modes and Von Mises stress

Figure 9(a) shows plastification at the joint in a 244.48 mm column with 7.1 mm thickness. In Figure 9(b), with 14.2 mm thickness, failure shifted to the lower flange of the beam.

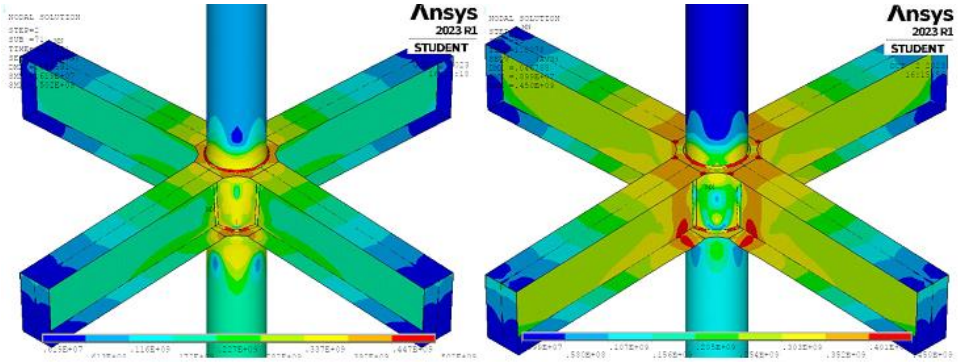


Figure 9. Von Mises stress at joint region

In Figures 10(a) and 10(b), the situation is somewhat different. Due to the large cross-section of the column, with a diameter of 355.6 mm, the diaphragm had less area to support the required loads, and the accumulation of loads was more concentrated in the lower part of the diaphragm and on the column wall. Note that the von Mises price is concentrated in this region. The failure mode occurs in the lower ring of the diaphragm. The thicknesses are the same as in the previous model: 7.1 mm and 14.2 mm, respectively.

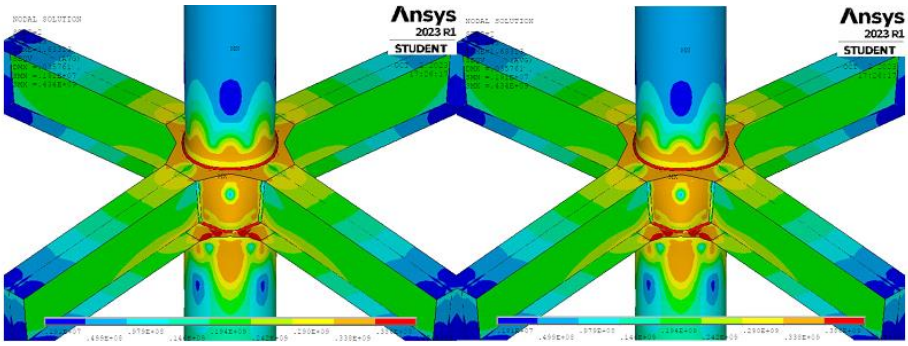


Figure 10. Von Mises stress and plastification

As thickness increases, failure shifts from the column face to other components such as the beam flange or diaphragm ring. Table 3 summarizes all failure locations.

Table 3. Failure modes for various diameters and thicknesses

THICKNESS	FAILURE MODES DIAMETERS			
	244,48	273	323,8	355,6
7,1	PP	PP	PP	PP
8	PP	PP	PP	PP
8,8	PP	PP	PP	PP
9,65	PP	PP	PP	PP
10	PP	PP	PP	PP
11	PP	PP	PP	PV
11,65	PP	PP	PV	PV
12,5	PP	PP	PV	PV
13,06	PP	PP	PV	PV
14,2	PV	PV	PV	PV

Where PP refers to plastification on the face of the column, and PV refers to plastification of both the beam flange and the diaphragm ring in the connection region. A total of 28 scenarios were analyzed, and 70% of the failures occurred in the column connection region, meaning the column was subjected to significant bending moments. In the remaining cases, failure occurred because the beam was unable to withstand the bending moment applied to it. From the experiment, we can infer that the larger the diameter, the greater the load-bearing capacity of the connection.

4 Conclusion

The external diaphragm connection performed satisfactorily, significantly increasing stiffness and strength under applied loads. In the first analysis stage (axial loading), the diaphragm-free model matched Winkel's results, while diaphragm-equipped models showed average displacements under 5 mm and over 50% gain in compressive strength.

In the second stage (combined loading), the diaphragm-enhanced models had superior structural performance, as confirmed by axial vs. displacement and moment vs. rotation graphs.

In the final stage, increased column wall thickness improved flexural strength and changed failure modes. Smaller sections failed at the column; larger sections failed at the beam or diaphragm. The results provide a consistent understanding of how external diaphragms and geometric parameters influence connection behavior.

5 Bibliographic references

[1] ASSOCIAÇÃO BRASILEIRA DE NORMAS TÉCNICAS. NBR 16239: Projeto de estruturas de aço e de estruturas mistas de aço e concreto de edificações com perfis tubulares. Rio de Janeiro, 2013.

[2] WINKEL, G. D. The static strength of I-beam to circular hollow section column connections. Tese (PhD) – Faculty of Civil Engineering and Geosciences, Delft University of Technology, Delft, Netherlands, 1998, p. 136.

[3] PEREIRA, D. H. F. Análise do comportamento estrutural de ligações em aço entre viga de seção I e pilar de seção tubular circular. 2013. Dissertação (Mestrado em Engenharia de Estruturas) – Escola de Engenharia de São Carlos, Universidade de São Paulo, São Carlos, 2013.

[4] ORRICO, A. C. R. S. Análise da influência do diafragma externo na ligação entre viga de seção I E pilar tubular de seção circular. 2018. Dissertação (Mestrado em Engenharia Civil) – Universidade Federal do Espírito Santo, Vitória, 2018.

[5] COUTINHO, F. G. Comportamento estrutural de ligações de aço com diafragma externo entre viga de seção I e pilar tubular de seção circular. 2015. Dissertação (Mestrado em Engenharia) – Universidade Federal do Espírito Santo, Vitória, 2015.

[6] KUROBANE, Y.; PACKER, J. A.; WARDENIER, J.; YEOMANS, N. CIDECT Design Guide 9: Design guide for structural hollow section column connections. Köln: CIDECT and Verlag TÜV Rheinland, 2004.